Title
Enhanced paramagnetism of TiBe2 and ferromagnetic transitions in TiBe2-xCux

Journal
Journal of Magnetism and Magnetic Materials, 22(3)

ISSN
0304-8853

Authors
Acker, F
Fisk, Z
Smith, JL
et al.

Publication Date
1981-02-01

DOI
10.1016/0304-8853(81)90029-9

Journal of Magnetism and Magnetic Materials 22 (1981) 250–256

ENHANCED PARAMAGNETISM OF $TiBe_2$ AND FERROMAGNETIC TRANSITIONS IN $TiBe_{2-x}Cu_x$

F. ACKER *, Z. FISK
Institute for Pure and Applied Physical Sciences **, *University of California, San Diego, La Jolla, CA 92093, USA*

J.L. SMITH and C.Y. HUANG
Los Alamos Scientific Laboratory ***, *Los Alamos, NM 87545, USA*

Received 19 August 1980

The magnetic behavior of $TiBe_2$ is found to be similar to that of strongly enhanced paramagnets like Pd and Ni_3Ga. The susceptibility curves $\chi(H, T = 0)$ and $\chi(T, H = 0)$ both go through a smooth maximum, at 55 kOe and 10 K, respectively, which might be due to the electron–electron interaction. For $TiBe_{2-x}Cu_x$ compounds the transition from paramagnetism to ferromagnetism is analyzed, starting from Arrott plots of the magnetization. A critical concentration $x_{cr} = 0.155 \pm 0.005$ is obtained. The Stoner–Edwards–Wohlfarth model of itinerant-electron magnetism is well followed near x_{cr}. The low temperature behavior of the specific heat of $TiBe_2$ is tentatively ascribed to the effect of the electron–phonon interaction on the electronic specific heat coefficient γ.

1. Introduction

There remains some uncertainty in the nature of the magnetism of $TiBe_2$. First, Enz and Matthias rightly predicted [1] that this compound would show itinerant-electron magnetism, since it is isostructural and isoelectronic with the weak ferromagnet $ZrZn_2$. The susceptibility of $TiBe_2$ was indeed found [2] to be very large ($\chi \approx 10^{-2}$ emu/mol, at $T = 0$) and to show a smooth maximum at 10 K, very like the one observed for Pd near 80 K. Because of the negative intercept of the extrapolated $\chi^{-1}(T)$ curve for $TiBe_2$ (Pd features that as well) the compound was labelled antiferromagnetic. This choice still influences the present research and leads to difficulties that will be mentioned below. By contrast, starting from the idea that $TiBe_2$ is a strongly enhanced paramagnet, the occurrence of ferromagnetism in $Ti_{1-x}Cu_xBe_2$ was predicted [3] and found [4] in $TiBe_{2-x}Cu_x$. However, the antiferromagnetic interpretation for $TiBe_2$ survived [5–8], calling for more experimental evidence.

Here we present and analyze detailed magnetic data for $TiBe_2$ (in particular high field measurements up to 213 kOe) and for $TiBe_{2-x}Cu_x$ (emphasizing the magnetic transition at x_{cr}). Earlier measurements of the specific heat [9] of $TiBe_2$, which play an important role in recent interpretations [5,7], are also discussed and compared with the results for Pd [10, 11].

* Partially supported on a grant from the Swiss National Science Foundation. Present address: Institut de Physique Experimentale, Université de Lausanne, 1015 Dorigny, Switzerland.
** Research in La Jolla supported by the National Science Foundation under Grant No. DMR77-08469.
*** Work at Los Alamos was performed under the auspices of the Department of Energy. Part of this work was performed while the authors were Guest Scientists at the Francis Bitter National Magnet Laboratory, which is supported at M.I.T. by the National Science Foundation.

2. Experimental techniques

The preparation of the compounds has been described earlier [4]. Measurements of the magnetization were made in three apparatuses. A Faraday balance was used to measure the susceptibility in a wide range of temperature (0.8–300 K). The high field measurements were carried out with a very low frequency vibrating sample magnetometer [12] at the

Francis Bitter National Magnet Laboratory. The magnetic transitions in $TiBe_{2-x}Cu_x$ were studied from data taken with a vibrating sample magnetometer where the specimen is held in thermal equilibrium with a large Cu block. This allows the temperature of the sample to be easily controlled (within $\Delta T < 10^{-2}$ K between 1.4 and 20 K). Detailed measurements (to 0.1%) of the low field susceptibility of $TiBe_2$ were also taken with this magnetometer. Using the four-probe ac technique the electrical resistance of a $TiBe_2$ sample was measured between 1.27 K and room temperature with a relative precision of 3×10^{-4}.

3. Results and discussion

3.1. Magnetic behavior of $TiBe_2$

The magnetic susceptibility, χ, of $TiBe_2$ was measured between 0.8 and 300 K. Fig. 1 shows the low field ($H < 10$ kOe) results for $T < 80$ K and a large scale plot of the data below 22 K. At the lowest temperature, the magnetic susceptibility of $TiBe_2$ is about 12 times larger than that of Pd. From 0.8 to 10 K, $\chi(T)$ increases by about 3% and then decreases steadily. No magnetic transition is suggested. The curves labelled A, B, C and D are calculated and will be described in section 3.3.

Above 50 K, the Curie–Weiss law is only followed in first approximation by the inverse susceptibility.

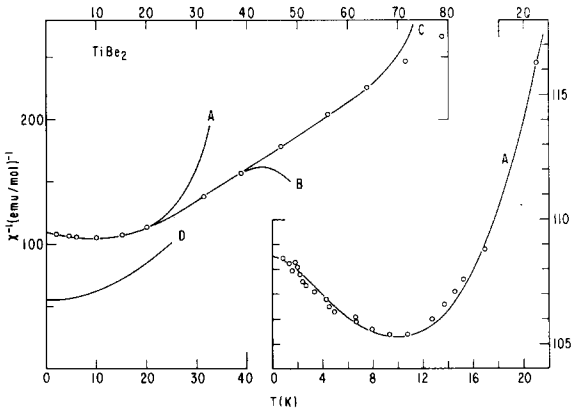

Fig. 1. Inverse magnetic susceptibility of $TiBe_2$ as a function of temperature. Curves A, B and C are fits to various orders to the Fermi liquid model. Curve D, see text.

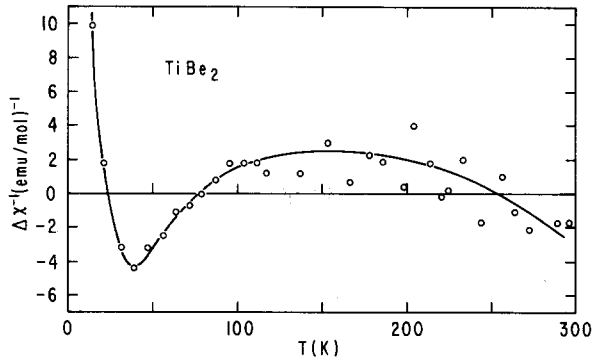

Fig. 2. Deviation of the inverse susceptibility of $TiBe_2$ from a least squares fit to the Curie–Weiss law, as a function of temperature.

The $\chi^{-1}(T)$ plot is slightly curved downwards. This nonlinearity is apparent in fig. 2 where $\Delta\chi^{-1}(T) = \chi^{-1}(T) - \chi_f^{-1}(T)$ is plotted versus T. Here χ_f^{-1} is the least squares fit of the data points above 20 K, $\chi_f^{-1} = 2.640(T + 22.3)$. The tangent at 250 K to the $\chi^{-1}(T)$ curve gives a Curie–Weiss temperature $\theta = -26.6$ K while the tangent at 50 K points to $\theta = -17.9$ K.

In fig. 3 the curve labelled $x = 0$ shows the variation of the magnetic susceptibility of $TiBe_2$ with the external field up to 213 kOe, at 1.24 K. A maximum in $\chi = M/H$ is found at $H_{max} \approx 55$ kOe. Between $H = 0$ and H_{max}, χ increases by 38%. The same data are plotted as M^2 vs H/M in fig. 4. This Arrott plot does not become linear even in the highest fields available and shows a characteristic right turn in the low field region.

3.2. Magnetic behavior of $TiBe_{2-x}Cu_x$ compounds

If Cu is partially substituted for Be in $TiBe_2$, the susceptibility gradually increases and ferromagnetism may be observed. We report here on systematic measurements of the magnetization of four $TiBe_{2-x}Cu_x$ samples with $x = 0.05, 0.10, 0.16$ and 0.20. Data were taken in order to determine whether a critical concentration for ferromagnetism, x_{cr}, could be defined and to find the behavior of $\chi(x, T)$ and $T_c(x)$ (Curie temperature).

The use of Arrott plots of the magnetization is known to be the best way to deal with nearly- or weakly-ferromagnetic substances for which $M(H)$ is nonlinear. Fig. 5 shows such a plot for $TiBe_{1.8}Cu_{0.2}$.

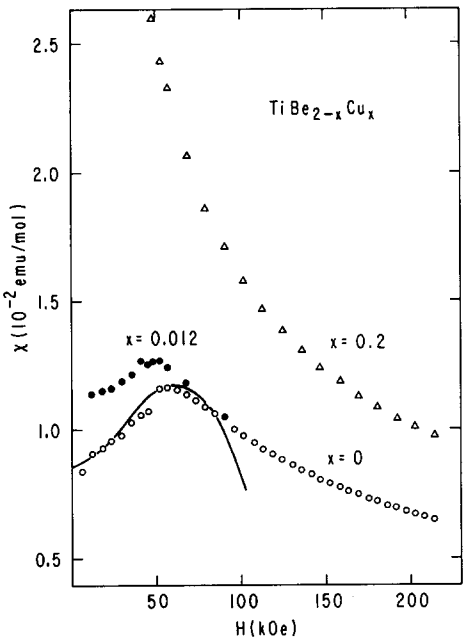

Fig. 3. Magnetic susceptibility of $TiBe_2$, $TiBe_{1.988}Cu_{0.012}$ and $TiBe_{1.8}Cu_{0.2}$ as a function of the external field at 1.24 K. The solid curve is the lowest order fit to the Fermi liquid model.

Parallel straight lines are obtained in moderate fields (1–10 kOe) and at low temperature. Deviations due to the magnetic inhomogeneity of the sample are

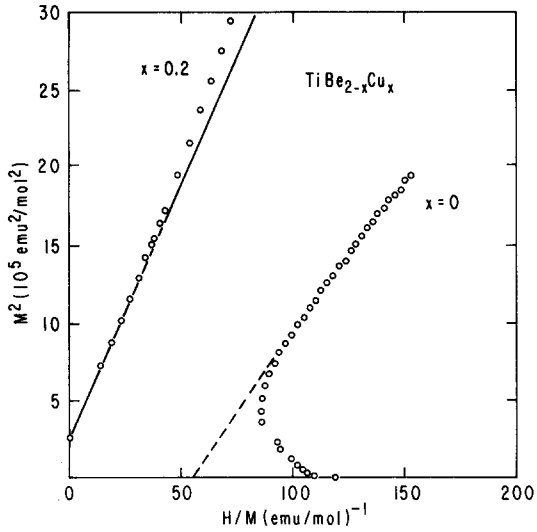

Fig. 4. Arrott plot (M^2 vs. H/M) in fields up to 213 kOe for $TiBe_2$ at 1.24 K. The plot for $TiBe_{1.8}Cu_{0.2}$ at 1.24 K is shown up to 120 kOe.

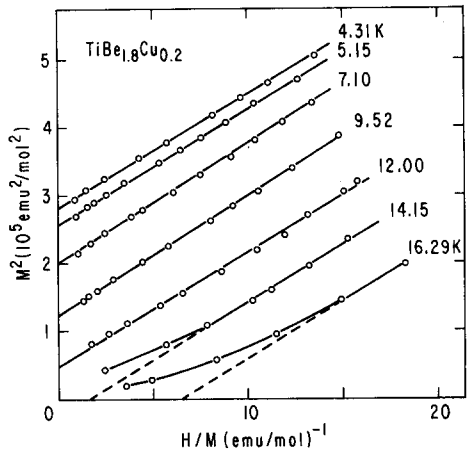

Fig. 5. Arrott plots (M^2 vs. H/M) for $TiBe_{1.8}Cu_{0.2}$ at various temperatures.

apparent above T_c. A reliable value of T_c can be obtained by plotting the values of $H/M \equiv \chi^{-1}$ extrapolated to $M^2 = 0$, as a function of T^2. This was done on fig. 6, for the four compounds studied. In first

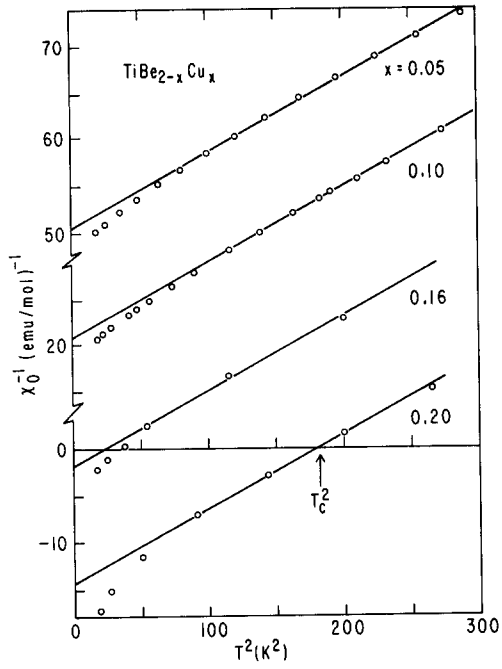

Fig. 6. Inverse magnetic susceptibility of $TiBe_{2-x}Cu_x$ compounds for x = 0.05, 0.10, 0.16 and 0.20 as a function of the square of the temperature.

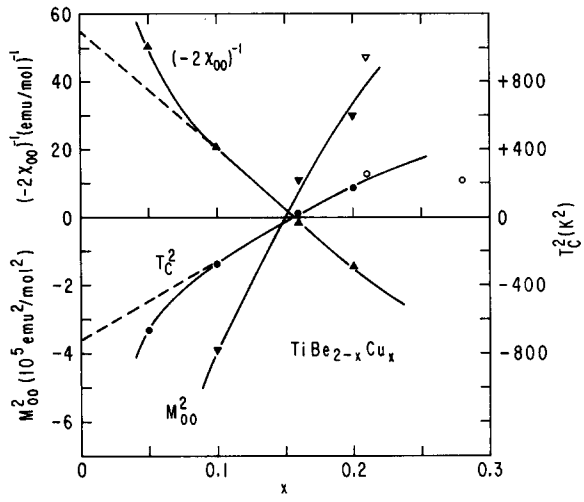

Fig. 7. Variation of the parameters $(-2\chi_{00}^{-1})$, T_c^2 and M_{00}^2 versus the Cu concentration for $TiBe_{2-x}Cu_x$ compounds. The open symbols are from ref. [4].

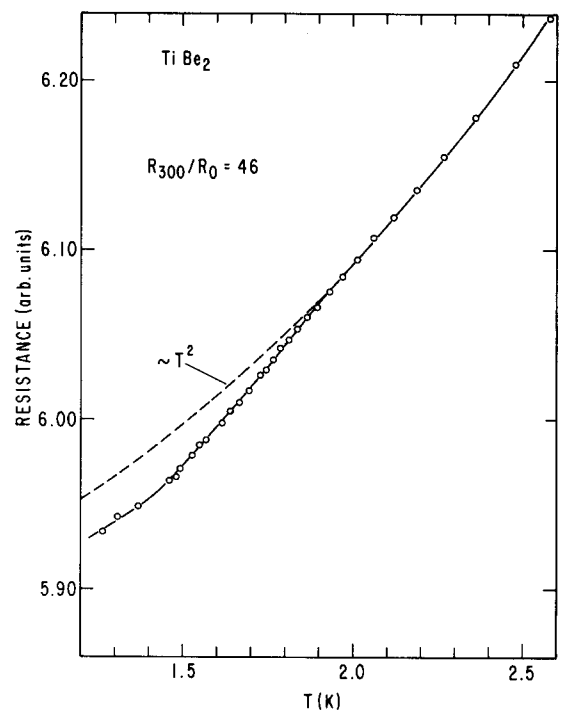

Fig. 8. Electrical resistance of $TiBe_2$ as a function of temperature.

approximation the data points define a set of parallel straight lines which cut the horizontal axis at T_c^2. By extrapolation, a (squared) Curie temperature may be formally defined for the paramagnetic compounds ($T_c^2 < 0$). See ref. [13] for more details about this analysis which is based on the Stoner–Edwards–Wohlfarth model of itinerant-electron magnetism [14]. The values of the inverse susceptibility extrapolated to $T = 0$ are deduced from fig. 6 and are denoted $(-2\chi_{00})^{-1}$. The zero field, zero temperature squared magnetization M_{00}^2 is obtained from the Arrott plots. In the present analysis, the magnetization $M(H, T)$ is described by the relation

$$M^2/M_{00}^2 = 1 - T^2/T_c^2 + 2\chi_{00}H/M\,,$$

where the characteristic quantities $T_c^2(x)$, $\chi_{00}^{-1}(x)$ and $M_{00}^2(x)$ all change sign at the critical concentration x_{cr}. From fig. 7, we obtain $x_{cr} = 0.155 \pm 0.005$.

The high field data for $TiBe_{1.988}Cu_{0.012}$ and $TiBe_{1.8}Cu_{0.2}$ were included in figs. 3 and 4, to allow for comparison with the behavior of $TiBe_2$. For x as low as 0.012 there is a significant shift, ($\approx -8 \pm 2$) kOe of the location of the maximum in χ (fig. 3). From a linear extrapolation H_{max} should be zero for $x = 0.07 \pm 0.02$. For $TiBe_{1.8}Cu_{0.2}$ the susceptibility decreases steadily with H from $H = 0$. An Arrott plot of the magnetization of this ferromagnetic sample deviates from linearity in high fields. It should be noted that this is not the same sample as in fig. 5. The $TiBe_{1.8}Cu_{0.2}$ sample of fig. 4 has its Curie point at 10 K and the slope of M^2 vs. H/M is larger in fig. 4 than in fig. 5. Thus the change of slope of the Arrott plot between $TiBe_2$ and $TiBe_{1.8}Cu_{0.2}$ should be analyzed with caution.

The low temperature part of our resistance measurements is shown in fig. 8. The resistance ratio $R(300\text{ K})/R(0)$ for this $TiBe_2$ sample is 46. Between 2 and 3 K the resistance varies like T^2. Above 3 K a T^n law with $n < 2$ is followed. No detailed measurements were taken above 4.2 K. A slight anomaly is observed in $R(T)$ around 1.8 K. Below 1.5 K the T^2 law appears to be obeyed.

3.3. Discussion

The data presented above all favor the paramagnetic interpretation for $TiBe_2$. The magnitude of the susceptibility, its smooth variation and the nonlinearity of $\chi^{-1}(T)$ are characteristic of the enhanced

paramagnetism found in substances like Pd, YCo_2, $LuCo_2$, etc. More strikingly, these materials share a remarkable property with $TiBe_2$: their magnetic susceptibility increases with both temperature and field, at low temperature [15–18]. At higher temperature $\chi(T)$ goes through a maximum. This can be explained by the Fermi liquid model [16–18] which further predicts a maximum in $\chi(H)$. We believe that $TiBe_2$ is the first compound where both maxima are clearly seen, at $T_{max} = 10$ K and $H_{max} = 55$ kOe. (For comparison, $T_{max} = 250$ K for YCo_2; the low temperature susceptibility of this compound bends over above 200 kOe but the maximum is not yet reached at 400 kOe [18].) In fact, Ni_3Ga [19,20] first showed such a behavior. Here, unfortunately, the maxima are obscured by an antagonist effect apparently due to magnetic impurities (the presence of 5 ppm Fe can account for it). It seems very likely that for pure and well ordered Ni_3Ga, $\chi(H)$ would show a maximum around 40 kOe and that $\chi(T)$ would decrease below 10–20 K. The similarity in the magnetic behavior of $TiBe_2$ and Ni_3Ga is made even clearer by comparing the values of the low temperature susceptibility, $\chi = 1.65 \times 10^{-2}$ emu/mol for Ni_3Ga [19] and $\chi = 0.90 \times 10^{-2}$ emu/mol for $TiBe_2$. The comparison may be extended to the temperature variation of χ or to the shape and slope of the Arrott plots (field variation).

The introduction of a few atomic percent of impurities in Pd and the deviation from stoichiometry in Ni_3Ga tend to suppress the maxima in $\chi(T)$ or $\chi(H)$ [17]. A corresponding behavior is observed for $TiBe_{2-x}Cu_x$ where both maxima disappear for an extrapolated $x \approx 0.07$.

The relative smallness of H_{max} and T_{max} in $TiBe_2$ makes this compound the ideal candidate for a detailed study of the surface $\chi(H, T)$ [18], in order to check the adequacy of the description based on the Fermi liquid model. We attempted to fit the data shown in figs. 1 and 3 to this model. Curves A, B and C were calculated, using the expression [17]

$$\chi(T) - \chi(0) = \sum_{\alpha=1}^{n} C_\alpha T^{\alpha+1} \ln(T/T_\alpha) ,$$

with $n = 1$, 2 and 3, respectively. The curve A ($\chi - \chi(0) = -bT^2 \ln(T/T_1)$) gives an excellent fit of the low temperature data and deviates from the experimental curve above $T \approx 2T_m$ [17]. A fit of $\chi(H)$ to the lowest order ($\chi - \chi(0) = -cH^2 \ln(H/H_1)$) is shown by the solid curve in fig. 3. The coefficients b and c, which are related to the enhancement factor S [17,20], are both positive here ($b = 5.7 \times 10^{-6}$ emu/mol K^2, $c = 1.9 \times 10^{-6}$ emu/mol kOe^2).

The study of the magnetic transition in $TiBe_{2-x}Cu_x$ brings further support to the paramagnetic interpretation for $TiBe_2$. Fig. 7 shows that the transition from paramagnetism to ferromagnetism at $x = 0.155$ can be well described by the Stoner–Edwards–Wohlfarth (SEW) model of itinerant-electron magnetism. The Landau parameter $A \equiv \chi_0^{-1}$ appearing in the equation of state $H = AM + BM^3$ is written as $A = \alpha T^2 + \beta(x_{cr} - x)$. Around x_{cr} this T^2 law is obeyed, in first approximation, as shown in fig. 6. The value of α is practically the same for all the samples and there is no indication of a transition to antiferromagnetism at $x = 0.155$. The present analysis makes use of the data taken in a "significant" low temperature range. The use [6] of higher temperature susceptibility data in order to define a Curie–Weiss temperature, θ, is not advisable here since θ has no meaning for an enhanced paramagnet. Note the parabolic variation of T_c with x above x_{cr} and the negative values of T_c^2 below x_{cr}, in our analysis.

The deviation from the SEW model which occurs below $x \approx 0.1$ seems to be related to the appearance of the maxima in $\chi(T)$ and $\chi(H)$. If the linear variation with x of the characteristic parameters $(-2\chi_{00})^{-1}$ and T_c^2 is extrapolated to $x = 0$, this gives $\chi^{-1}(T = 0) = 55$ (emu/mol)$^{-1}$ and $T_c^2 = -720$ K^2 for $TiBe_2$. The figure for the susceptibility compares surprisingly well with the value found by a tentative extrapolation to $H = 0$ of the high field Arrott plot for $TiBe_2$ in fig. 4. Using $\chi^{-1}(0) = 55$ and $T_c^2 = -720$ the curve labelled D in fig. 1 was obtained. The difference between curve D and the experimental curve may be viewed as an effect of the electron–electron interaction.

3.4. Discussion of the specific heat results

It appears that the unifying theoretical ideas expressed by Enz [21] about itinerant magnetism and superconductivity could well accomodate a strongly paramagnetic (nearly ferromagnetic) $TiBe_2$. (In ref. [21] the "antiferromagnetism" was even

viewed as a complication.) Nevertheless, efforts were made [7] to find evidence for antiferromagnetism from the specific heat data which show a low temperature upturn and an intriguing cusp around 2 K [9]. This was done in spite (because [7]) of the fact that no clue for antiferromagnetism can be found from the magnetic behavior of $TiBe_2$ [5,7]. Assuming that spin density wave (SDW) antiferromagnetism occurs in $TiBe_2$, "phasons" were made responsible for the specific heat anomaly. As already outlined in ref. [7], this interpretation bears several difficulties. We shall just mention them here: i) The sharp kink observed in C/T vs. T^2 is not well fitted by a phason term, which has the form of a shoulder. ii) No critical temperature for the SDW can be found from susceptibility measurements (but it was loosely meant [7] that $T_m \approx 10$ K = T_{max} in our notation). iii) The specific heat discontinuity associated with the disappearance of the SDW at T_m is not detected around 10 K or elsewhere. iv) The specific heat cusp at 2 K is still present in the ferromagnetic $TiBe_{2-x}Cu_x$ compounds, where the SDW should, in principle, disappear.

The analogy of $TiBe_2$ with Pd suggests a simpler explanation which is consistent with the magnetic data. Due to the electron–phonon interaction, the coefficient γ of the electronic specific heat might vary considerably with T, at low temperature. As shown in fig. 9, the decomposition of the specific heat C_V of Pd into a Debye function and a γT term with θ_D and γ both constant is impossible. In analyzing the same data, Veal and Rayne [12] chose to keep γ constant and were left with an increasing $\theta_D(T)$. On the other hand, Clusius and Schachinger [11] noticed earlier that after subtraction of a contribution $\gamma(T)\,T = \alpha\chi(T)\,T$ the specific heat of Pd can be described by a nearly constant value of θ_D, up to room temperature.

The curves shown in fig. 9 were obtained by subtracting Debye terms with various fixed values of θ_D to the experimental data. They are strongly reminiscent of the curve computed (before the fact) by Grimvall [22] for the temperature variation of γ due to the electron–phonon interaction. A low temperature upturn of $\gamma(T)$ below $T \approx 100$ K and a maximum around $T = 20$ K is thus very likely for Pd. For $TiBe_2$, sticking to the analogy with Pd, one may expect to see a similar upturn of C/T vs. T^2 and possibly a maximum. The fact that the maxima are located at $T \approx$

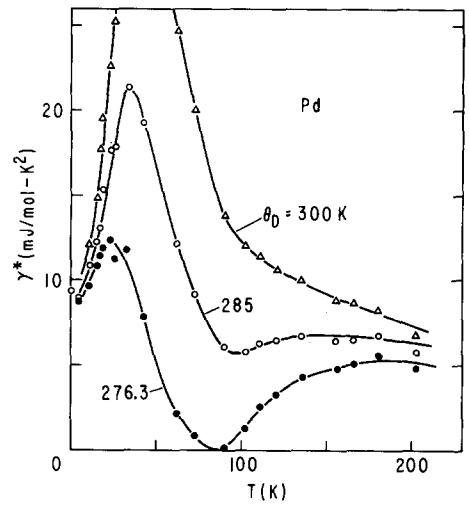

Fig. 9. Electronic specific heat coefficient γ^* of Pd as a function of temperature. γ^* was obtained by subtracting a Debye contribution $f_D(\theta_D/T)$ from the experimental C_V data, for various values of θ_D. The experimental C_V values below 25 K are from ref. [12] and above 25 K from ref. [11].

$T_m/4$ in both materials might be fortuitous and would require further analysis. The behavior of θ_D in $TiBe_2$ and $TiBe_{2-x}Cu_x$ should be studied by higher temperature specific heat measurements.

Although the entropy associated with the specific heat anomaly appears to be too large to be accounted for by the presence of an impurity phase this explanation cannot be ruled out a priori. Since $TiBe_3$ forms in the center of the grains there could be a superconducting Ti-rich phase (maybe even β-Ti) at the grain boundaries. Specific heat measurements in a magnetic field might clarify this point. A more remote possibility could be the presence of Magneli phases Ti_nO_{2n-1} [23–25] with $n \geqslant 6$. By analogy with V_nO_{2n-1} [26] these still little studied oxides might show large peaks in the specific heat at low temperature, due to metal–insulator transitions.

The resistivity ratio $R(300\text{ K})/R(0) = 46$ that we found in $TiBe_2$ indicates a high purity. The low temperature data in fig. 8 show the characteristic T^2 variation already found in $ZrZn_2$ [27] and Ni_3Al [28]. The anomaly observed near 1.8 K is very small and its possible connection with a maximum of $\gamma(T)$ at the same temperature or with the presence of an impurity phase should be investigated.

4. Conclusion

A coherent picture of the magnetic properties of $TiBe_2$ has been given. $TiBe_2$ is found to be a strongly exchange-enhanced paramagnet and to behave in every respect like Pd or Ni_3Ga. The electron–electron interaction can be made responsible for the maxima found in $\chi(T)$ and $\chi(H)$. The low temperature behavior of the specific heat is tentatively attributed to a temperature dependence of the electronic specific heat coefficient γ due to the electron–phonon interaction.

The transition between paramagnetism and ferromagnetism in $TiBe_{1-x}Cu_x$ takes place at the critical concentration $x_{cr} = 0.155 \pm 0.005$. Around x_{cr}, the Stoner–Edwards–Wohlfarth model of itinerant-electron magnetism is well followed. No transition to antiferromagnetism could be detected below x_{cr} by our measurements.

The analogies between $TiBe_2$ and Pd suggest further experiments. The possible inducement of giant moments in $TiBe_2$ by Fe or Ni impurities should be investigated. In spite of the fact that the occurrence of superconductivity is not favored by the high susceptibility of the material, the effect of H impurities or irradiation should also be checked. A study of the specific heat below 1.5 K and above 25 K would be of interest and might clarify the origin of the anomaly at 2 K.

Note added in proof

Recent measurements of the specific heat of $TiBe_2$ by L.D. Woolf (private communication) show no peak around 1.8 K. Instead, C/T decreases regularly, by about 8%, when T^2 increases from 0.5 to 5.0 K^2. In the discussion of the susceptibility results we should have mentioned the theoretical result of Beal-Monod et al. who find no $T^n \ln T$ terms (see Phys. Rev. B21 (1980) 5400). According to Doniach and Engelsberg (Phys. Rev. Lett. 17 (1966) 750) $T^3 \ln T$ terms should be present in the specific heat of strongly enhanced paramagnets.

References

[1] C.P. Enz and B.T. Matthias, Science 201 (1978) 828.
[2] B.T. Matthias, A.L. Giorgi, V.O. Struebing and J.L. Smith, J. de Phys. Lett. 39 (1978) L441.
[3] F. Acker, unpublished analysis of the data of ref. [2].
[4] A.L. Giorgi, B.T. Matthias, G.R. Stewart, F. Acker and J.L. Smith, Solid State Commun. 32 (1979) 455.
[5] C.P. Enz, in: Proc. 1980 Intern. Symp. on Atomic, Molecular and Solid State Theory, eds. P.-O. Löwdin and Y. Öhrn, Intern. J. Quantum Chem. 46 (1980) to be published.
[6] C.P. Enz and B.T. Matthias, Merz Fesch. J. of Ferroelectrics, to be published.
[7] C.P. Enz and G.R. Stewart, to be published.
[8] R.A. de Groot, D.D. Koelling and F.M. Mueller, J. Phys. F Lett., to be published.
[9] G.R. Stewart, B.T. Matthias, A.L. Giorgi, E.G. Szklarz and J.L. Smith, Solid State Commun. 30 (1979) 709.
[10] K. Clusius and L. Schachinger, Z. Naturforsch. 2a (1947) 90.
[11] B.W. Veal and J.A. Rayne, Phys. Rev. 135 (1964) A442.
[12] S. Foner and E.J. McNiff, Jr., Rev. Sci. Instr. 39 (1968) 171.
[13] F. Acker and R. Huguenin, J. Magn. Magn. Mat. 12 (1979) 58.
[14] D.M. Edwards and E.P. Wohlfarth, Proc. Roy. Soc. (London) A303 (1968) 127.
[15] E.A. Mueller, R. Gersdorf and L.W. Roeland, Phys. Lett. 31A (1970) 424.
[16] S. Misawa, Phys. Rev. Lett. 26 (1971) 1632.
[17] G. Barnea, J. Phys. C8 (1975) L216.
[18] S. Misawa, J. Phys. F8 (1978) L263.
[19] C.J. Schinkel, F.R. de Boer and B. de Hon, J. Phys. F3 (1973) 1463.
[20] G. Barnea and D.M. Edwards, J. Phys. F7 (1977) 1323.
[21] C.P. Enz, in: Superconductivity in d- and f-Band Metals, eds. H. Suhl and M.B. Maple (Academic Press, New York, 1980).
[22] G. Grimvall, J. Phys. Chem. Solids 29 (1968) 1221.
[23] L.K. Keys and L.N. Mulay, Japan. J. Appl. Phys. 6 (1967) 122.
[24] W.J. Danley and L.N. Mulay, Mater. Res. Bull. 7 (1972) 739.
[25] M. Marezio, D. Tranqui, S. Lakkis and C. Schlenker, Phys. Rev. B16 (1977) 2811.
[26] D.B. McWhan, J.P. Remeika, J.P. Maita, H. Okinaka, K. Kosuge and S. Kachi, Phys. Rev. B7 (1973) 326.
[27] S. Ogawa, Physica 91B (1977) 82.
[28] J.H.J. Fluitman, R. Boom, P.F. de Châtel, C.J. Schinkel, J.L.L. Tilanus and B.R. de Vries, J. Phys. F3 (1973) 109.